DOI: 10.1002/ejic.200800345

Hydrogen Bonding and Anion Binding in Structures of Tris(pyrazolyl)boratenickel(II) and Phosphate Esters

M. Dolores Santana,*[a] Luisa López-Banet,[a] Gabriel García,[a] Luís García,[b] José Pérez,*[b] and Malva Liu[c]

Keywords: Hydrogen bonds / Nickel / NMR spectroscopy / Receptors / Solid-state structures / Phosphates

This paper presents the syntheses, crystal structures and spectroscopic properties of a series of nickel(II) complexes containing hydrotris(3,5-dimethylpyrazolyl)borate and phosphate esters: $[Tp^*Ni(Hpz^*)_2(L)][(RO)_2PO_2]$ [R = Et, Bu; L = H_2O (**1**), $(BuO)_2P(O)OH$ (**2**)] and $[Tp^*Ni(Hpz^*)(H_2O)_2][(EtO)_2PO_2]$ (**5**) {Tp^* = hydrotris(3,5-dimethylpyrazolyl)borate, Hpz^* = 3,5-dimethylpyrazole}. The complexes $[Ni(Tp^*)_2]$ (**3**) and $[(Tp^*Ni)_2(\mu\text{-}pz^*)(\mu\text{-}OH)]$(**4**) were also prepared and fully characterized. X-ray crystallographic studies of **1** and **2** reveal that the pyrazole moieties are hydrogen bonded to the guest phosphate ester anion. In complex **5**, the phosphate anion is hydrogen-bonded by two O–H groups of the water molecules. Their behavior in solution was investigated by 1D and 2D ^1H NMR spectroscopic techniques.

Introduction

The design and synthesis of anion receptors or sensors have attracted considerable attention due to the importance of anions in biological and environmental systems.[1] Among these endeavors, the development of selective receptors for phosphate anions is of particular interest, because they play vital roles in a wide range of live processes.[2] However, the design of effective receptors is a challenging task because of the intrinsic properties of the phosphate ion. The incorporation of transition metals into the synthesis of anion receptors set up a new way in this area.[3] The reaction between a transition-metal ion and a phosphorus acid or ester has attracted the attention of inorganic, bioinorganic, biological, and material chemists in view of its relevance in metal-catalyzed phosphate ester hydrolysis,[4] the synthesis of cage-like and extended framework phosphates,[5] and the generation of single molecular magnets.[6] An interesting and common fact in metal phosphates is the presence of a certain number of hydrogen bonds, which often contributes to a great extent to the understanding of the associated chemistry. In particular, the H-bonding found in metal phosphates has recently clarified the mechanism of metal-assisted phosphate ester hydrolysis.[7] It is well-demonstrated that bulky alkyl or aryl substituents on phosphate ligands can act as monodentate ligands leaving the phosphoryl P=O group free, which results in the formation of interesting intra- and intermolecular hydrogen-bonding networks in the solid state and in solution.[8] In an attempt to expand this area of chemistry, we selected tris(3,5-dimethylpyrazolyl)borate (Tp*) as an ancillary ligand for nickel(II), specifically to study their reactivity towards phosphorus acids. The hydrotris(pyrazolyl)borate ligand (Tp^R) is widely used in the design of functional molecules, catalysis of asymmetric synthesis, molecular "electronic devices", and biomimetic chemistry.[9] The least-hindered hydrotris(pyrazolyl)borate ligands Tp and Tp* have a strong tendency to form stable and inert full-sandwich complexes $[M^{II}Tp_2^R]$; however, it is relatively difficult to obtain half-sandwich mononuclear complexes.[10] Recently, some methods to synthesize half-sandwich complexes have been reported.[11] In this paper, we prepared mononuclear half-sandwich nickel(II) complexes that contain the hydrotris(3,5-dimethylpyrazolyl)borate ligand (Tp*) and one or two Hpz* molecules that are coordinated to nickel ions and ester phosphate anions. The aforementioned complexes could be useful precursors for the rational synthesis of small molecular building blocks that might lead to higher ordered structures that are prepared under conventional conditions. These complexes were studied by IR, NMR, and UV/Vis spectroscopy, mass spectrometry, and X-ray crystallography.

Results and Discussion

Synthesis of the Complexes

Mononuclear nickel complexes $[Tp^*Ni(Hpz^*)_2(L)][(RO)_2PO_2]$ (R = Et, Bu) containing one Tp* ligand, two Hpz*

[a] Departamento de Química Inorgánica, Universidad de Murcia, 30071 Murcia, Spain
E-mail: dsl@um.es
[b] Departamento de Ingeniería Minera, Geológica y Cartográfica, Área de Química Inorgánica, Universidad Politécnica de Cartagena, 30203 Cartagena, Spain
[c] Departament de Termodinámica, Universitat de València, 4 6100 Burjassot, València, Spain

moieties, and one H_2O (**1**) or $(BuO)_2P(O)OH$ (**2**) molecules were synthesized upon addition of the corresponding phosphoric acid $[(RO)_2P(O)OH]$ to a $CHCl_3$ solution of [NiCl(Tp*)]·(Hpz*) and aqueous NaOH, followed by extraction into hexane. The syntheses of **1** and **2** were accompanied by a partial hydrolysis of the tris(pyrazolyl)borate ligand and the coordination of the released pyrazole into the nickel ions. This event has been observed in complexes with tris(pyrazolyl)borate ligands containing Ni^{II}[9,12] or Cu^{II} ions.[13]

The reaction of KTp* in THF with $NiCl_2·6H_2O$ in MeOH produced two products. The first one is a violet precipitate that could be crystallized and formulated as $[Ni(Tp^*)_2]$ (**3**). After handing the filtrate, the second product was isolated in good yield as a green solid that was identified as $[(Tp^*Ni)_2(\mu\text{-}pz^*)(\mu\text{-}OH)]$ (**4**). The reaction of **4** with $[(EtO)_2P(O)OH]$ in CH_2Cl_2 at room temperature gave a blue complex identified as $[Tp^*Ni(Hpz^*)(H_2O)_2]$-$[(EtO)_2PO_2]$ (**5**).

Structural Description

The structures of all complexes were determined by single-crystal X-ray diffraction. Selected bond lengths and angles are given in Table 1 and structural parameters are summarized in Table 2. The Ni^{II} ion in **1** is coordinated to five nitrogen atoms and one oxygen atom to form a distorted N_5O octahedron. Three nitrogen atoms come from the Tp* ligand and two from the Hpz* moiety; the oxygen atom comes from a water molecule. The average bond lengths of Ni–N(Tp*) and Ni–N(Hpz*) are 2.089 and 2.137 Å, respectively. These Ni–N bond lengths are typical for a $TpNi^{II}$ center.[9] The bond length of Ni–OH_2 is 2.117(2) Å. The strongest bound pyrazole of the Tp* ligand is *trans* to the water molecule N1–Ni1–O1 178.38(7)°. In **1**, two phosphate anions link two complexes by hydrogen bonds forming a "dimeric" unit that exhibits C_2 symmetry. There are eight hydrogen bonds in the "dimer", in which the N atoms from the Hpz* moiety and the O atoms from the water molecules are involved (Figure 1). In contrast, complex **2** has a molecule of dibutyl phosphoric acid as a monodentate ligand (Figure 2). The Ni^{II} ion in **2** is coordinated to five nitrogen atoms, three from the Tp* ligand and two from the Hpz* unit, and one oxygen atom from a dibutyl phosphoric acid, and together they form the N_5O octahedral environment. The average bond lengths of Ni–N(Tp*) and Ni–N(Hpz*) are 2.107 and 2.141 Å, respectively. The bond length of Ni–O1 $[(BuO)_2P(O)OH]$ is 2.077(2) Å. The shortest bond Ni–N(Tp*) is *trans* to the neutral dibutyl phosphoric acid O1–Ni1–N5 174.33(7)°. In **2**, each cationic complex is linked to a phosphate anion by three hydrogen bonds, where the N atoms from the Hpz* ligands and the OH group from the phosphoric acid are involved (Figure 2).

The structure of **3** consist of centrosymmetric $[Ni(Tp^*)_2]$ units (Figure 3). The coordination environment of the Ni^{II} atom in **3** is a N_6 octahedron built by two κ^3 coordinate Tp* ligands. All the bond lengths and angles in the Tp* ligands are normal, and the average bond lengths of Ni–N(Tp*) is 2.128 Å, similar to those previously observed in the bis[hydrotris(3-Me-pyrazol-1-yl)borate]nickel(II) complex.[14] The ORTEP view of **4** is presented in Figure 4. The complex adopts a dinuclear structure (C_2 symmetry) bridged with one pyrazole ligand and one hydroxido ligand, in which each metal ion is five-coordinate with a N_4O ligand-donor set. The coordination geometry of each nickel ion could be better described as a distorted square pyramid (τ = 0.29).[15,16] The Ni–N(Tp*) distances are not significantly different (2.027–2.111 Å) and are similar to the Ni–N(pz*) distance (2.047 Å). These bond lengths are typical of five-coordinate $(Tp)Ni^{II}$ derivatives that show distorted square pyramidal geometry.[17–19] The Ni–O bond length is 1.949(2) Å as that previously found for a five-coordinate nickel complex.[20] In complex **4**, bridging ligands define a five-membered ring. The probabilistic classification method developed by the authors[21] yield probabilities of 0.778 and 0.222 for *half-chair* and *envelope* conformations, respectively.

The structure of **5** contains $[Tp^*Ni(Hpz^*)(H_2O)_2]^+$ units (Figure 5). The nickel atoms are coordinated to three nitrogen atoms from the Tp* unit, one nitrogen atom from the Hpz* ligand, and two oxygen atoms from the water molecules; together they form the N_4O_2 octahedral environment. The average bonds lengths of Ni–N(Tp*) and Ni–N(Hpz*) are 2.081 and 2.106(4) Å, respectively. The bond lengths of

Table 1. Selected bond lengths [Å] and angles [°] for complexes **1**–**5**.

	1	2	3	4	5
Ni1–N1	2.0659(18)	2.1079(18)	2.142(2)	2.066(2)	2.067(5)
Ni1–N3	2.1141(18)	2.1293(18)	2.106(2)	2.027(2)	2.070(5)
Ni1–N5	2.0864(18)	2.0845(19)	2.137(2)	2.111(2)	2.107(4)
Ni1–N7	2.1439(18)	2.1315(18)		2.0466(19)	2.105(4)
Ni1–N9	2.1290(18)	2.1513(19)			
Ni1–O1	2.1176(16)	2.0765(16)		1.9486(12)	2.058(5)
Ni1–O2					2.135(5)
N1–Ni1–N3	90.99(7)	85.71(7)	91.33(8)/ 88.67(8)	92.00(8)	90.9(2)
N1–Ni1–N5	89.81(7)	89.60(7)	92.24(8)/ 87.76(8)	83.50(8)	87.00(19)
N1–Ni1–N7	88.37(7)	171.98(7)		96.37(8)	92.9(2)
N1–Ni1–N9	89.07(7)	90.27(7)			
N1–Ni1–O1	178.38(7)	92.10(7)		153.88(6)	176.8(2)
N3–Ni1–N5	84.61(7)	88.87(7)	89.00(8)/ 91.00(8)	90.85(8)	88.80(17)
N3–Ni1–N7	172.17(7)	86.96(7)		97.63(8)	93.53(18)
N3–Ni1–N9	87.09(7)	175.31(7)			
N3–Ni1–O1	90.57(7)	96.65(6)		113.83(6)	90.2(2)
N5–Ni1–N7	87.59(7)	93.52(7)		171.52(7)	177.67(18)
N5–Ni1–N9	171.61(7)	88.69(7)			
N5–Ni1–O1	89.67(7)	174.33(7)		91.95(8)	90.05(18)
N7–Ni1–N9	100.69(7)	97.19(7)			
N7–Ni1–O1	90.07(7)	85.50(6)		84.44(9)	89.99(19)
N9–Ni1–O1	91.67(7)	85.90(7)			
N1–Ni1–O2					89.1(2)
N3–Ni1–O2					178.4(2)
N5–Ni1–O2					89.64(19)
N7–Ni1–O2					88.0(2)
O1–Ni1–O2					89.7(2)

Table 2. Crystal data and summary of data collection and refinement for complexes **1**–**5**.

Complex	**1**	**2**	**3**	**4**	**5**
Empirical formula	$C_{29}H_{50}BN_{10}NiO_5P$	$C_{41}H_{75}BN_{10}NiO_8P_2$	$C_{30}H_{44}B_2N_{12}Ni$	$C_{35}H_{52}B_2N_{14}Ni_2O$	$C_{24}H_{44}BN_8NiO_6P$
M	719.28	967.57	653.10	823.95	641.16
T [K]	100(2)	100(2)	100(2)	100(2)	293(2)
λ [Å]	0.71073	0.71073	0.71073	0.71073	0.71073
Crystal system	monoclinic	monoclinic	triclinic	monoclinic	monoclinic
Space group	$C2/c$	$P2_1/n$	$P\bar{1}$	$C2/c$	$C2/c$
a [Å]	26.0983(11)	14.0512(8)	8.5162(4)	17.1015(11)	20.8090(7)
b [Å]	10.0978(4)	19.9559(11)	10.7910(5)	13.9912(9)	14.4910(4)
c [Å]	27.6453(11)	17.8989(10)	10.9534(5)	16.9602(11)	22.6860(8)
α [°]	90	90	115.3490(10)	90	90
β [°]	100.5500(10)	99.6320(10)	98.4710(10)	91.2990(10)	107.4630(10)
γ [°]	90	90	109.0930(10)	90	90
V [Å^3 [Å]	7162.4(5)	4948.2(5)	809.51(6)	4057.0(5)	6525.5(4)
Z	8	4	1	4	8
$D_{calcd.}$ [g cm^{-3}]	1.334	1.299	1.340	1.349	1.305
μ [mm^{-1}]	0.638	0.515	0.641	0.976	0.692
$F(000)$	3056	2072	346	1736	2720
θ range for data collection [°]	1.50 to 28.20	1.79–28.20	2.18–28.14	1.88–28.21	1.74–27.52
Reflections collected	40084	56431	9446	22970	11143
Independent reflections	8331, R_{int} = 0.0262	11418, R_{int} = 0.0311	3627, R_{int} = 0.0154	4702, R_{int} = 0.0205	7249, R_{int} = 0.0596
Goodness-of-fit on F^2	0.983	1.013	1.075	1.074	1.006
Final R indices[a,b] [$I > 2\sigma(I)$]:	R_1 = 0.0469,	R_1 = 0.0464,	R_1 = 0.0520,	R_1 = 0.0479,	R_1 = 0.0824,
R_1 = 0.0464,	wR_2 = 0.1310	wR_2 = 0.1296	wR_2 = 0.1475	wR_2 = 0.1339	wR_2 = 0.2232
wR_2 = 0.1296					
R indices (all data)[a,b]	R_1 = 0.0511,	R_1 = 0.0547,	R_1 = 0.0529,	R_1 = 0.0508,	R_1 = 0.1829,
	wR_2 = 0.1347	wR_2 = 0.1361	wR_2 = 0.1483	wR_2 = 0.1373	wR_2 = 0.2876
Max/min $\Delta\rho$ [e Å^{-3}]	1.025/–0.667	1.099/–0.629	0.646/–0.864	1.534/–0.621	0.949/–0.669

[a] $R_1 = \Sigma||F_o| - |F_c||/\Sigma|F_o|$ for reflections with $I > 2\sigma I$. [b] $wR_2 = \{\Sigma[w(F_o^2 - F_c^2)^2]/\Sigma[w(F_o^2)^2]\}^{1/2}$ for all reflections; $w^{-1} = \sigma^2(F^2) + (aP)^2 + bP$, in which $P = (2F_c^2 + F_o^2)/3$ and a and b are constants set by the program.

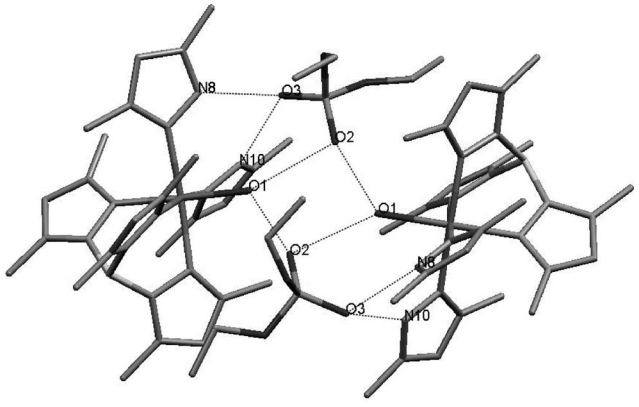

	d(D–H) [Å]	d(H···A) [Å]	<(D–H···A) [°]	d(D···A) [Å]
O1–H37···O2#1	0.83	1.89	166.4	2.706(3)
O1–H38···O2#2	0.73	2.16	171.0	2.884(3)
N8–H39···O3#2	0.89	1.83	165.6	2.697(2)
N10–H40···O3#2	0.86	1.87	165.2	2.709(3)

#1: 0.5 – x, y – 1/2, –z + 1/2; #2: x + 1/2, y – 1/2, z

Figure 1. Structural parameters for H-bonds in complex **1**.

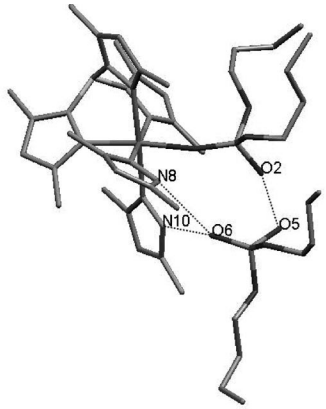

	d(D–H) [Å]	d(H···A) [Å]	<(D–H···A) [°]	d(D···A) [Å]
N10–H73···O6	0.81	2.12	158.0	2.889(2)
N8–H74···O6	0.80	2.12	148.0	2.830(2)
O2–H75···O5	0.99	1.43	172.0	2.413(2)

Figure 2. Structural parameters for H-bonds in complex **2**.

Ni–O(H_2O) are 2.072(4) and 2.137(5) Å, respectively. In **5**, two phosphate anions link two complexes by hydrogen bonds, which form a "dimeric" unit that exhibits C_2 symmetry. There are six hydrogen bonds in the "dimer", and water molecules (but not Hpz*) are implicated in them (Figure 5). In relation to the conformation adopted by the Tp* ligand coordinated to the Ni^{II} ion, there are three six-membered BN_2NiN_2 rings in each complex reported in this paper. The conformation of each ring was evaluated by using the probabilistic classification method.[21] All of them adopt a slightly distorted *boat* conformation (the method yields a probability close to 1.0 for every ring) and the deviation from the boat theoretical torsion angles ranges is between 7.7 and 14.6°. The average bond lengths (Ni–N and Ni–O) of these complexes became shorter with the increasing numbers of coordinated oxygen atoms (see Table 1). The

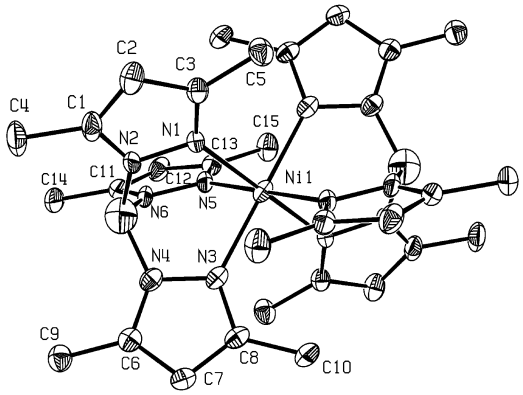

Figure 3. ORTEP drawing of the cation of complex **3** (ellipsoids at 50% probability level) with atom-labeling scheme.

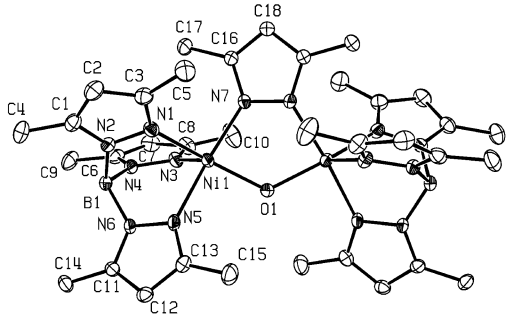

Figure 4. ORTEP drawing of the cation of complex **4** (ellipsoids at 50% probability level) with atom-labeling scheme.

nickel(II) ion has an N_6-coordinate environment in **3**, N_5O-coordinate environment in **1** and **2**, N_4O_2-coordinate environment in **5**, and finally, the five-coordinate environment of **4** is N_4O. A comparison between the Ni–N(Hpz*) distances of **1**, **2**, and **5** shows a lengthening of the distances for the pyrazole ligands involved in the hydrogen bonding of the phosphate ester anions (see Table 1).

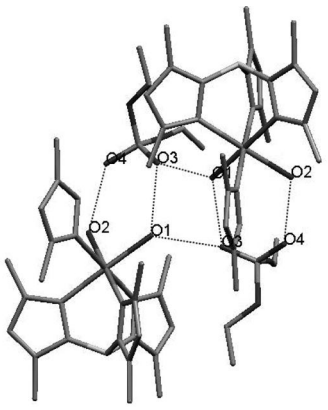

	d(D–H) [Å]	*d*(H···A) [Å]	<(D–H···A) [°]	*d*(D···A) [Å]
O1–H31···O3	0.77	1.98	153.4	2.686(7)
O2–H33···O4#3	0.85	1.80	158.6	2.609(9)
O1–H32···O3#3	0.69	2.00	175.0	2.689(8)

#3: $-x + 1, y, -z + 1/2$

Figure 5. Structural parameters for H-bonds in complex **5**.

Spectroscopic Properties

Characterization of complexes **1**–**5** by IR spectroscopy reveals B–H stretches between 2513–2509 cm^{-1}, a fact that is indicative of κ^3 coordination of the Tp* ligands.[22] The IR spectra of **1**, **2**, and **5** also exhibit two bands due to $\nu_{as}(PO_2)$ and $\nu_s(PO_2)$ vibrations in the 1208–1202 and 1067–1044 cm^{-1} ranges, respectively. The bands in the 1184–1164 and 980–952 cm^{-1} regions could be assigned to the ν[(P)–O–C] and ν[P–O-(C)] vibrations, respectively.[23] The bands of ν(N–H) at 3195, 3192, and 3187 in the spectra of **1**, **2**, and **5**, respectively, indicate the Hpz* ligation.

Paramagnetic ^1H NMR spectra were recorded for complexes **1**–**5**. The ^1H NMR spectra of these paramagnetic high-spin nickel(II) complexes are useful for assessing to what extent the solid-state structures are maintained in solution. The NMR peaks for these nickel(II) compounds were assigned on the basis of their chemical shift, relative integration, longitudinal relaxation times (T_1), observed {^1H–^1H} COSY and {^1H–^1H} NOESY cross peaks, and comparisons with previously reported tris(pyrazolyl)borate compounds.[18] In all cases, the Tp* arms are magnetically equivalent in solution. The assignment process of the resonances of $[Tp^*Ni(Hpz^*)_2(H_2O)][(EtO)_2PO_2]$ (**1**) in $CDCl_3$ is discussed as a representative example (Figure 6). In the spectrum of **1**, the peak with the largest downfield shift (58.5 ppm) has an integration of 3 protons and a short T_1 (1.5 ms); it was assigned to the 4-H of the pyrazolyl ring of Tp*, in accordance with the observed properties of the 4-H protons of the pyrazolyl ring in other $Ni(Tp^{R1,R2})$ complexes.[18,20] In general, the nearest protons to the nickel(II) ion suffer the largest chemical shift and the greatest line broadening. The 5-methyl protons of Tp* near the boron atom (T_1 = 2.9 ms) were less upfield shifted (≈ –1.2 ppm) than the 3-methyl protons of the Tp* ligand near the nickel ion (–9.8 to –9.7 ppm). In complexes **1** and **2**, the 4-H-pz* proton appears at 25.4 and 25.5 ppm, respectively. The methyl protons of the pyrazole groups are observed at 16.4 and 16.2 ppm (3-Me) and the resonances of 5-Me-Hpz* (≈ –1.2 ppm) are overlapped by the 5-Me-Tp* ligand. The resonances of the alkyl groups of the phosphate esters furthest from the nickel atom have the smallest shift with regard to the diamagnetic position and all these resonances are downfield. The resonances of the ethyl phosphate protons of **1** are assigned to the remaining unassigned peaks at 3.7 and 1.4 ppm. Relative integrations require that the peak at 3.7 ppm correspond to the -OCH_2 protons, so the remaining three-proton resonance at 1.4 ppm must be assigned to the methyl protons. Complex **2** exhibits similar ^1H NMR shift patterns and relaxation parameters (Figure 7), although new resonances appear at 3.6, 1.8, 1.3, and 0.8 ppm,

which can be assigned to the butyl (-OCH_2, -CH_2–CH_2-, and -CH_3) protons, respectively. The connectivity between the latter four is established by observation of the {^{1}H–^{1}H} COSY spectrum (Figure 8). The paramagnetic shift falls off and the relaxation time increases with the distance between the nickel(II) center and the butyl phosphoric protons, a fact that indicates a dominant σ-bond spin delocalization pathway.[24] In **4**, the situation is more complex and the resonances are assigned on the basis of its integration, T_1, and the solid-state structure. Thus, the peaks at 75.7 (1 H), 48.9 (2 H), and 44.5 (4 H) ppm are assigned to the 4-H of bridging-pz*, 4-H-Tp*(ax), and 4-H-Tp*(eq) protons, respectively, rendering all three pyrazolyl rings from Tp* inequivalent, and therefore, twofold symmetry could be maintained in solution. The 3- and 5-methyl protons appear in three groups (as the 4-H protons) with 2:2:4 ratios that correspond to bridging, axial, and equatorial pyrazolyl rings. The behavior of **4** toward $(EtO)_2P(O)OH$ was investigated by titration in $CDCl_3$ and followed by ^{1}H NMR spectroscopy (Figure 9). These results show visible changes in the spectrum; thus, after the addition of equimolar amounts of the phosphoric acid, only resonances corresponding to each of the 3-, 4-, and 5-H protons of Tp* are observed. These experimental results could indicate the lack of a symmetry plane due to phosphate binding. ^{1}H NMR signals observed for **5** can be assigned on the basis of signal intensity and the assignment of **1** and **2**. The resonances of 4-H-Tp* (59.2 ppm) and 4-H-pz* (39.6 ppm) have larger downfield shifts in **5** than in complexes **1** and **2**, as is evidenced by the fact that the Ni–N bond lengths in the solid-state structure are shorter for this complex and Hpz* is not involved in hydrogen bonding to the phosphate ester anion. The {^{1}H–^{1}H} NOESY spectrum (Figure 10) also shows remarkably clear cross peaks between 4-H-Tp* (59.2 ppm), -OCH_2 (3.8 ppm), and -CH_3 (1.4 ppm) from the ethyl phosphate protons. Furthermore, clear NOE cross signals are observed between resonances at 3.8, 1.4, and –1.3 ppm (Figure 10 inset), and the last signal can be assigned to the overlapped 5-Me-Tp* + 5-Me-Hpz* protons. This assignment is consistent with the solid-state structure, which

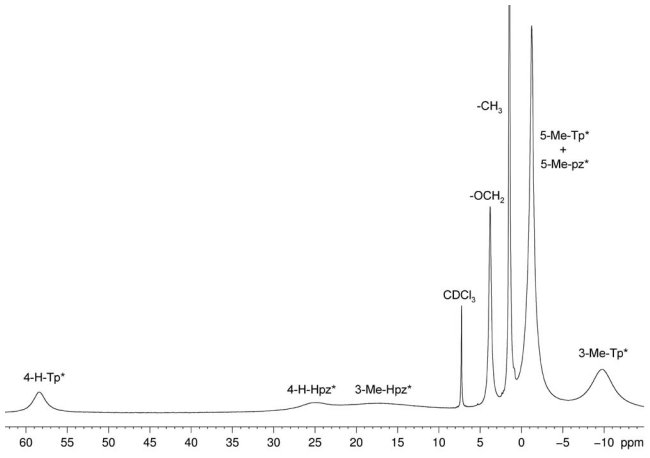

Figure 6. ^{1}H NMR spectrum of **1** (in $CDCl_3$ solution at room temperature).

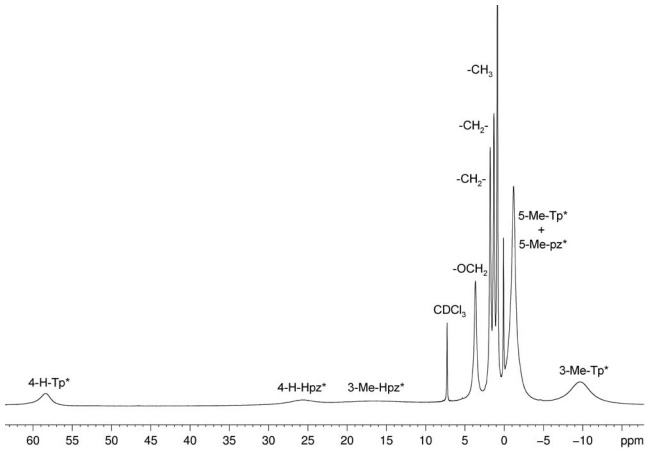

Figure 7. ^{1}H NMR spectrum of **2** (in $CDCl_3$ solution at room temperature).

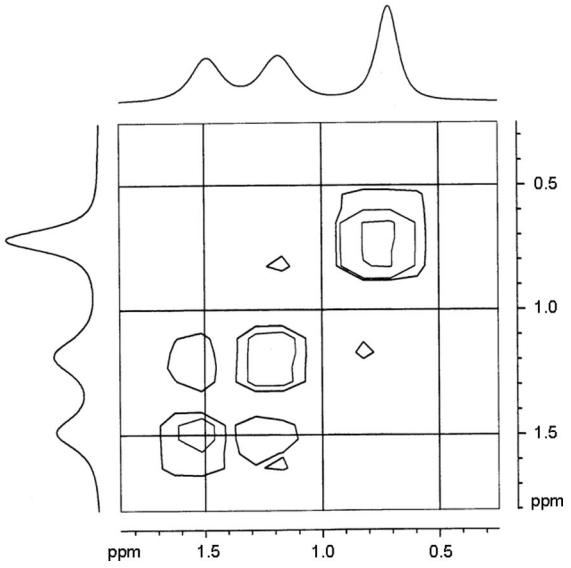

Figure 8. Portion of the {^{1}H–^{1}H} COSY spectrum of complex **2** (in $CDCl_3$ solution at 20 °C). Only the relevant region to assign phosphate resonances is shown in the top trace.

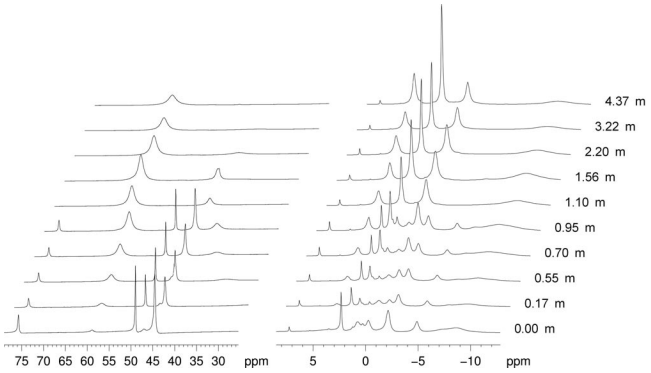

Figure 9. ^{1}H NMR spectrum of **4** (0.049 M in $CDCl_3$) upon successive addition of $(EtO)_2P(O)OH$ at room temperature.

shows the spatial proximity between all these groups, and therefore, the anion binding found in the solid state could be maintained in the solution structure.

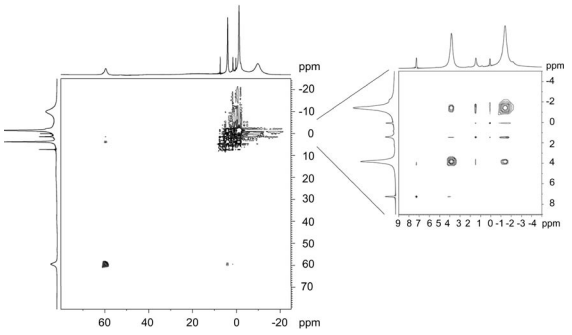

Figure 10. {^{1}H–^{1}H} NOESY spectrum of complex **5** (in $CDCl_3$ solution at 21 °C). The relevant region to assign the ethyl phosphate and methyl resonances is shown in the inset.

Conclusions

In this paper, we prepared three nickel(II) complexes containing hydrotris(3,5-dimethylpyrazolyl)borate and phosphate esters: [Tp*Ni(Hpz*)$_2$(L)][(RO)$_2$PO$_2$] {R = Et, Bu; L = H_2O (**1**), $(BuO)_2P(O)OH$ (**2**)}, and [Tp*Ni(Hpz*)-(H_2O)$_2$][(EtO)$_2$PO$_2$] (**5**). The complexes [Ni(Tp*)$_2$] (**3**) and [(Tp*Ni)$_2$(μ-pz*)(μ-OH)](**4**) were also prepared and fully characterized. The phosphate binding through two pyrazole moieties by hydrogen bonding was found in the solid-state structure of **1** and **2**. In complex **5**, the phosphate anion was hydrogen bonded by two O–H groups of the water molecules. The anion binding was investigated in solution by 1D and 2D ^{1}H NMR spectroscopic techniques.

Experimental Section

Materials and Physical Measurements: The KTp* ligand and [NiCl(Tp*)]·(Hpz*) were synthesized according to literature methods.[25,19,26] Their purity was confirmed by MS (FAB) and ^{1}H NMR spectroscopy. Other chemicals were reagent grade and used as received. The C, H, and N analyses were performed with a Carlo Erba model EA 1108 microanalyzer. The ^{1}H NMR spectra were recorded with Bruker spectrometers (AC 200E or AC 300E) by using $SiMe_4$ as a standard. The magnitude {^{1}H–^{1}H} COSY spectrum was recorded with a Bruker 200 MHz spectrometer at 20 °C in $CDCl_3$ solution by using 256 individual FIDs with 4096 scans each and the repetition time was 150 ms. The {^{1}H–^{1}H} NOESY spectra was recorded with a Bruker 200 MHz spectrometer at 21 °C in $CDCl_3$ solutions by using 256 individual FIDs with 2048 scans each. The mixing time was varied in the 30–150 ms range. Presaturation of 1.4 ppm resonance was applied during both relaxation delay and mixing time. Experimental parameters were varied to obtain best resolution and signal to noise. Oven-dried 5-mm NMR tubes were filled with a solution of **4** (0.049 M in $CDCl_3$). After recording the NMR spectrum of **4**, successive aliquots of $(EtO)_2$-P(O)OH (in $CDCl_3$) separately prepared were injected through the septum. Infrared spectra were recorded with a Perkin–Elmer 16F PC FTIR spectrophotometer by using Nujol mulls between polyethylene sheets. MS (ESI) analyses were performed with an Agilent VL mass spectrometer. The ionization mechanism used was electrospray in negative ion full scan mode by using methanol/ammonium acetate as the solvent (for **5** the solvent was $CHCl_3$) and nitrogen gas for desolvation, except for **4**, which the ionization mechanism used was electrospray in positive ion full scan mode. The UV/Vis spectra (in CH_2Cl_2) were recorded with a UNICAM 520 spectrophotometer equipped with matched quartz cells in the 300–800 nm range. The chemicals were purchased from Aldrich and used without further purification. Solvents were dried and distilled by general methods before use.

Synthesis of [Tp*Ni(Hpz*)$_2$(H_2O)][(EtO)$_2$PO$_2$] (1) and {Tp*Ni-(Hpz*)$_2$[(BuO)$_2$P(O)OH]}[(BuO)$_2$PO$_2$] (2): A solution of [NiCl-(Tp*)]·(Hpz*) (69 mg, 0.142 mmol) in toluene (10 mL) was stirred with aqueous NaOH (1 N, 2.4 mL) for 30 min. The toluene phase was separated, dried with $MgSO_4$, and filtered to eliminate the salt. After removal of the solvent under vacuum, the resulting solid was dissolved in $CHCl_3$ (10 mL) and the corresponding phosphoric acid $(RO)_2P(O)OH$ (0.215 mmol) was added to the solution and stirred for 0.5 h. The solution was reduced to dryness and stirred with hexane (5 mL). Recrystallization of the resulting solid from $CHCl_3$/hexane (1:5) and slow evaporation afforded **1** or **2** as blue microcrystals. Data for **1**: Yield: 44.1 mg (73%). $C_{29}H_{50}BN_{10}NiO_5P$ (719.26): calcd. C 48.43, H 7.01, N 19.47; found C 48.28, H 7.05, N 19.00. MS (ESI): *m*/*z* (%) = 813.6 (100) [M + Hpz*]. UV/Vis (CH_2Cl_2): λ (ε, $M^{-1}cm^{-1}$) = 633 (20), 401 (46) nm. IR (nujol): $\tilde{\nu}$ = 3604 (ν_{OH}), 3195 (ν_{NH}), 2513 (ν_{BH}), 1545 ($\nu_{C=N}$), 1202 (ν_{aPO_2}), 1164 [$\nu_{(P)-O-C}$], 1044 (ν_{sPO_2}), 959 [$\nu_{P-O-(C)}$] cm^{-1}. ^{1}H NMR (300 MHz, $CDCl_3$, TMS): δ = 58.5 (3 H, 4-H-Tp*), 25.4 (2 H, 4-H-pz*), 16.4 (6 H, Me-pz*), 3.7 (2 H, -OCH_2), 1.4 (3 H, -CH_3), –1.2 (15 H, 5-Me-Tp* + Me-pz*), –9.7 (9 H, 3-Me-Tp*) ppm. Data for **2**: Yield: 45.1 mg (52%). $C_{41}H_{75}BN_{10}NiO_8P_2$ (967.55): calcd. C 50.90, H 7.81, N 14.48; found C 50.62, H 7.78, N 14.85. MS (ESI): *m*/*z* (%) = 798.4 (54) [M – $(BuO)_2PO_2$ + K]. UV/Vis (CH_2Cl_2): λ (ε, $M^{-1}cm^{-1}$) = 636 (14), 399 (35) nm. IR (nujol): $\tilde{\nu}$ = 3192 (ν_{NH}), 2509 (ν_{BH}), 1544 ($\nu_{C=N}$), 1208 (ν_{aPO_2}), 1184 [$\nu_{(P)-O-C}$], 1067 (ν_{sPO_2}), 980 [$\nu_{P-O-(C)}$] cm^{-1}. ^{1}H NMR (200 MHz, $CDCl_3$, TMS): δ = 58.4 (3 H, 4-H-Tp*), 25.5 (2 H, 4-H-pz*), 16.3 (6 H, Me-pz*), 3.7 (2 H, -OCH_2), 1.8 (2 H, -CH_2-), 1.3 (2 H, -CH_2-), 0.8 (3 H, -CH_3), –1.2 (15 H, 5-Me-Tp* + Me-pz*), –9.7 (3 H, 3-Me-Tp*) ppm.

Synthesis of [Tp*$_2$Ni] (3) and [Tp*$_2$Ni$_2$(μ-pz*)(μ-OH)] (4): A solution of KTp* (2.5 g, 7.57 mmol) in THF (100 mL) was mixed with a solution of $NiCl_2$·$6H_2O$ (1.8 g, 7.57 mmol) in MeOH (20 mL), and the mixture was stirred for 20 min. The solution was filtered, and the resulting violet solid was then washed with water to eliminate the salt and then with hexane. Sparingly soluble product **3** was obtained as violet microcrystals from CH_2Cl_2/MeOH (Yield: 1.2 g, 24.3%). The filtrate was dried under vacuum to afford a pink powder, which was washed with hexane and ether. It was then dissolved in CH_2Cl_2, and the resulting solution was filtered and the solvents evaporated to dryness. The resultant powder was extracted with toluene (100 mL). Aqueous NaOH (1 N, 69 mL) was then added to this solution, and the mixture was stirred for 20 min. The toluene phase was separated, dried with $MgSO_4$, and then filtered. Evaporation of the solvent under vacuum followed by recrystallization of the resulting solid from hexane at 5 °C afforded **4** as green crystals (Yield: 0.82 g, 60.9%). Data for **3**: $C_{30}H_{44}B_2N_{12}Ni$ (653.07): calcd. C 55.17, H 6.79, N 25.74; found C 54.93, H 6.78, N 25.39. MS (ESI): *m*/*z* (%) = 653.2 (100) [M]. IR (nujol): $\tilde{\nu}$ = 2507 (ν_{BH}), 1542 ($\nu_{C=N}$) cm^{-1}. ^{1}H NMR (200 MHz, $CDCl_3$, TMS): δ = 52.1 (6 H, 4-H-Tp*), –2.1 (18 H, 5-Me-Tp*), –9.1 (18 H, 3-Me-Tp*) ppm. Data for **4**: $C_{35}H_{52}B_2N_{14}Ni_2O$ (823.89): calcd. C 51.02, H 6.36, N 23.80; found C 51.08, H 6.67, N 23.61. MS (ESI): *m*/*z* (%) = 769.1 (100) [M – pz* + K]. UV/Vis (CH_2Cl_2): λ (ε, $M^{-1}cm^{-1}$) = 626 (55),

391 (293) nm. IR (nujol): $\tilde{\nu}$ = 3705 (ν_{OH}), 2511 (ν_{BH}), 1544, 1522 ($\nu_{C=N}$) cm^{-1}. ^1H NMR (300 MHz, $CDCl_3$, TMS): δ = 75.7 (4-H-pz*), 48.9 (2 H, 4-H-Tp*), 44.5 (4 H, 4-H-Tp*), 2.3 (6 H, 5-Me-Tp*), –0.3 (6 H, 3-Me-Tp*), –2.1 (12 H, 5-Me-Tp*), –4.9 (6 H, Me-pz*), –8.8 (12 H, 3-Me-Tp*) ppm.

[Tp*Ni(Hpz*)(H_2O)$_2$][(EtO)$_2PO_2$] (5): A solution of **4** (100 mg, 0.121 mmol) and $(EtO)_2P(O)OH$ (37.3 mg, 0.242 mmol) in CH_2Cl_2 was stirred for 30 min. After removal of the solvent under vacuum, hexane was added, and the mixture was cooled to –30 °C. The resulting blue solid was collected by filtration, recrystallized from $CHCl_3$/hexane (1:5), and dried. Blue microcrystals were afforded by slow evaporation of a CH_2Cl_2 solution. Yield: 88.4 mg (57%). $C_{24}H_{44}BN_8NiO_6P{\cdot}CHCl_3$ (760.51): calcd. C 39.48, H 5.96, N 14.73; found C 39.60, H 6.27, N 14.68. MS (ESI): *m/z* (%) = 881.4 (100) [M + 2$CHCl_3$]. UV/Vis (CH_2Cl_2): λ (ε, $M^{-1}cm^{-1}$) = 643 (12), 401 (33) nm. IR (nujol): $\tilde{\nu}$ = 3626 (ν_{OH}), 3187 (ν_{NH}), 2506 (ν_{BH}), 1543 ($\nu_{C=N}$), 1203 (ν_{aPO_2}), 1164 [$\nu_{(P)-O-C}$], 1044 (ν_{sPO_2}), 952 [$\nu_{P-O-(C)}$] cm^{-1}. ^1H NMR (200 MHz, $CDCl_3$, TMS): δ = 59.2 (3 H, 4-H-Tp*), 39.6 (1 H, 4-H-pz*), 23.5 (3 H, Me-pz*), 3.8 (2 H, -OCH_2), 1.4 (3 H, -CH_3), –1.3 (12 H, 5-Me-Tp* + Me-pz*), –9.9 (9 H, 3-Me-Tp*) ppm.

Crystal Structure Determination: Data collection for **1**, **2**, **3**, and **4** was performed at –173 °C with a Bruker Smart CCD diffractometer with a nominal crystal to detector distance of 4.5 cm. Diffraction data were collected based on a ω scan run. A total of 2524 frames were collected at 0.3° intervals and 10 s per frame. The diffraction frames were integrated by using the SAINT package[27] and corrected for absorption with SADABS.[28] Data collection of **5** was performed at 293° K with a Nonius Kappa-CCD single crystal diffractometer. Crystal-detector distance was fixed at 35 mm, and a total of 122 images were collected by using the oscillation method, with scan angle per frame, 2° oscillation and 20 s exposure time per image. Data collection strategy was calculated with the program Collect.[29] Data reduction and cell refinement were performed with the programs HKL Denzo and Scalepack.[30] The structures were solved by direct methods[31] and refined by full-matrix least-squares techniques by using anisotropic thermal parameters for non-H atoms[31] (Table 2).

CCDC-681286 (for **1**), -681287 (for **2**), -681288 (for **3**), -681289 (for **4**), and -681290 (for **5**) contain the supplementary crystallographic data for this paper. These data can be obtained free of charge from The Cambridge Crystallographic Data Centre via www.ccdc.cam.ac.uk/data_request/cif.

Acknowledgments

We wish to thank Dr. A. Donaire for his valuable suggestions and to Dr. A. de Godos for recording the NMR spectra. This work was supported by the Dirección General de Investigación del Ministerio de Educación y Ciencia, Spain (Project No. CTQ2005-09231-C02-01). L. L.-B. thanks the Fundación Séneca for a FPI-grant.

[1] a) P. D. Beer, E. J. Hayes, *Coord. Chem. Rev.* **2003**, *204*, 167; b) M. J. Chmielewski, J. Jurczak, *Chem. Eur. J.* **2005**, *11*, 6080.
[2] Z. Chen, X. Wang, J. Chen, X. Yang, Y. Li, Z. Guo, *New J. Chem.* **2007**, *31*, 357.
[3] P. D. Beer, S. R. Bayly, *Top. Curr. Chem.* **2005**, *255*, 125.
[4] a) N. H. Williams, B. Takasaki, M. Wall, J. Chin, *Acc. Chem. Res.* **1999**, *32*, 485; b) P. E. Jurek, A. E. Martell, *Inorg. Chem.* **1999**, *38*, 6003.
[5] S. Neeraj, P. M. Forster, C. N. R. Rao, A. K. Cheetham, *Chem. Commun.* **2001**, 2716.
[6] E. K. Brechin, R. A. Coxall, A. Parkin, S. Parsons, P. A. Tasker, R. E. P. Winpenny, *Angew. Chem. Int. Ed.* **2001**, *40*, 2700.
[7] J. Chin, S. Chung, D. H. Kim, *J. Am. Chem. Soc.* **2002**, *124*,10948.
[8] R. Murugavel, M. Sathiyendiran, R. Pothiraja, R. J. Butcher, *Chem. Commun.* **2003**, 2546.
[9] Y.-J. Sun, W.-Z. Shen, P. Cheng, S.-P. Yan, D.-Z. Liao, Z.-H. Jiang, P.-W. Shen, *Polyhedron* **2004**, *23*, 211–218.
[10] S. Trofimenko, *Chem. Rev.* **1993**, *93*, 943.
[11] Y.-J. Sun, P. Cheng, S.-P. Yan, Z.-H. Jiang, D.-Z. Liao, P.-W. Shen, *Inorg. Chem. Commun.* **2000**, *3*, 289–291, and references therein.
[12] J. Kisala, Z. Ciunik, K. Drabent, T. Ruman, S. Wolowiec, *Polyhedron* **2003**, *22*, 1645–1652.
[13] L. M. L. Chia, S. Radojevic, I. J. Scowen, M. McPartlin, M. A. Halcrow, *J. Chem. Soc., Dalton Trans.* **2000**, 133–140.
[14] P. Cecchi, G. G. Lobbia, F. Marchetti, G. Valle, S. Calogero, *Polyhedron* **1994**, *13*, 2173–2178.
[15] A. W. Addison, T. N. Rao, J. Reedijk, J. van Rijn, G. C. Verschoor, *J. Chem. Soc., Dalton Trans.* **1984**, 1349–1356.
[16] In this convention, a square pyramid would have a τ value of 0.00, and a trigonal bipyramid would have a τ value of 1.00.
[17] T. Ruman, M. Łukasiewicz, Z. Ciunick, S. Wołowiec, *Polyhedron* **2001**, *20*, 2551.
[18] S. Hikichi, M. Yoshizawa, Y. Sasakura, H. Komatsuzaki, Y. Moro-oka, M. Akita, *Chem. Eur. J.* **2001**, *7*, 5011–5028.
[19] A. V. Yakovenko, S. V. Kolotilov, A. W. Addison, S. Trofimenko, G. P. A. Yap, V. Lopushanskaya, V. V. Pavlishchuk, *Inorg. Chem. Commun.* **2005**, *8*, 932–935.
[20] N. Kitajima, S. Hikichi, M. Tanaka, Y. Moro-oka, *J. Am. Chem. Soc.* **1993**, *115*, 5496–5508.
[21] M. Kessler, J. Pérez, M. C. Bueso, L. García, E. Pérez, J. L. Serrano, R. Carrascosa, *Acta Crystallogr., Sect. B* **2007**, *63*, 869–878.
[22] M. Akita, K. Ohta, Y. Yakamashi, S. Hikichi, Y. Moro-oka, *Organometallics* **1997**, *16*, 4121.
[23] a) P. N. Turowski, W. H. Armstrong, S. Liu, S. N. Brown, S. J. Lippard, *Inorg. Chem.* **1994**, *33*, 636–645; b) J. Pérez, L. García, R. Carrascosa, E. Pérez, J. L. Serrano, G. Sánchez, G. García, M. D. Santana, L. López, J. García, *Z. Anorg. Allg. Chem.* **2007**, *633*, 1869–1874.
[24] I. Bertini, C. Luchinat, *NMR of Paramagnetic Molecules in Biological Systems*, Benjamin/Cummings Publishing Co., Menlo Park, CA, **1986**.
[25] D. M. Eichhorn, W. H. Armstrong, *Inorg. Chem.* **1990**, *29*, 3607–3612.
[26] D. J. Harding, P. Harding, H. Adams, T. Tuntulani, *Inog. Chim. Acta* **2007**, *360*, 3335–3340.
[27] *SAINT*, Version 6.22, Bruker AXS, Inc.
[28] G. M. Sheldrick, *SADABS*, University of Gottingen, **1996**.
[29] *COLLECT*, Nonius BV, **1997–2000**.
[30] Z. Otwinowski, W. Minor, "DENZO-SCALEPACK: Processing of X-ray Diffraction Data Collected in Oscillation Mode" in *Methods in Enzymology Vol. 276: Macromolecular Crystallography, Part A* (Eds.: C. W. Carter Jr, R. M. Sweet), Academic Press, San Diego, **1997**, pp. 307–326.
[31] G. M. Sheldrick, *SHELX-97: Programs for Crystal Structure Analysis* (release 97–2), University of Göttingen, **1998**.

Received: April 4, 2008
Published Online: July 24, 2008

